*Thermal Science and Engineering (2023) Volume 6 Issue 2*
doi: 10.24294/tse.v6i2.2188

## ORIGINAL RESEARCH ARTICLE

# New multi-energy sources coupling a low-temperature sustainable central heating system with a multifunctional relay energy station

**Fangtian Sun[1,2,*], Xiaoqing Zhao[1], Wanqing Xu[1], Zhicheng Wang[1], Yonghua Xie[1]**

[1] *Department of Thermal Energy and Power Engineering, Beijing University of Civil Engineering and Architecture, Beijing 100044, China*

[2] *Beijing Research Center of Sustainable Energy and Buildings, Beijing University of Civil Engineering and Architecture, Beijing 100044, China*

*** Corresponding author:** Fangtian Sun, sun_fangtian@163.com

## ABSTRACT

Due to short cost-effective heat transportation distance, the existing geothermal heating technologies cannot be used to develop the deep hydrothermal type geothermal fields situated far away from urban area. To solve the problem, a new multi-energy source coupling a low-temperature sustainable central heating system with a multifunctional relay energy station is put forward. As for the proposed central heating system, a compression heat pump integrated with a heat exchanger in the heating substation and a gas-fired water/lithium bromide single-effect absorption heat pump in the multifunctional relay energy station are used to lower return temperature of the primary network step by step. The proposed central heating system is analyzed by using thermodynamics and economics, and matching relationships between design temperature of return water and main line length of the primary network are discussed. The studied results indicate that, as for the proposed central heating system, the cost-effective main line length of the primary network can approach 33.8 km, and the optimal design return temperature of the primary network is 23 °C. Besides, annual coefficient of performance and annual exergy efficiency of the proposed central heating system are about 3.01 and 42.7%, respectively.

***Keywords:*** low temperature central heating; hydrothermal type geothermal energy; compression heat pump; absorption heat pump; multifunctional relay energy station; multi-energy coupled operation

**ARTICLE INFO**

Received: 1 June 2023
Accepted: 17 July 2023
Available online: 7 August 2023



## 1. Introduction

Developing deep hydrothermal type geothermal resource for low temperature central heating contributes to achievement of carbon peaking & carbon neutrality[1,2]. In Northern China, the deep hydrothermal type geothermal energy is about $1.78 \times 10^9$ GJ per year, and it is available for space heating[3]. Space distribution of deep hydrothermal type geothermal energy is discontinuous due to complicated geotectonic movement over a long time scale[4,5]. In most cases, distances between the deep hydrothermal type geothermal field and the center of heat load are very long, and they are beyond upper-limit of cost-effective geothermal energy transportation distance of the convention geothermal central heating systems[6,7]. Therefore, lengthening cost-effective geothermal energy transportation distance is the key to the development of deep hydrothermal type geothermal fields, which is located far away from the center of heat load.

In comparison to the high-temperature central heating, the low-temperature sustainable central heating can utilize low-temperature geothermal energy efficiently[8–9]. As for the low temperature geothermal central heating system, enlarging temperature difference between supply water and return water of the primary network would decrease mass flow rate of circulating water, and it helps to reduce construction cost of the primary network and electricity consumption of circulating water pump. Thus, bigger temperature difference between supply and return of the primary network contributes to increasing CEGETD[10,11]. In the low-temperature sustainable central heating systems, reducing return temperature of the primary network can increase temperature difference between supply water and return water, and it also helps to utilize low-temperature heat efficiently[12]. Therefore, reducing return temperature of the primary network is a feasible measure to enlarge temperature difference between supply water and return water of the primary network.

To lower return temperature of the primary network, both the absorption heat exchanger[13,14] and the ejector heat exchanger[15] are presented, and they have been applied successfully in the heating substations of the high-temperature central heating systems driven by industrial waste heat. As for the absorption heat exchanger and the ejector heat exchanger, supply temperature of the primary network, must be higher than 120 ℃, and thus they are not suitable for the low temperature sustainable central heating systems. To reduce return temperature of the primary network in the industrial waste heat central heating systems, a compression heat pump integrated with a heat exchanger is proposed[16,17]. Concerning the compression heat pump integrated with a heat exchanger, low return temperature of the primary network would result in big ratio of outlet pressure to inlet pressure of the compressor, and its coefficient of performance (COP) would become small[18,19]. However, low return temperature of the primary network would contribute to decreasing power consumption of circulating water pumps in the primary network and utilizing low-temperature heat efficiently. Therefore, the design return temperature of the primary network should be optimized from the aspect of the whole system performance. So far, the research related to this topic has not been carried out.

On the other hand, the deep hydrothermal type geothermal energy is generally used to take on basic load for increasing utilization rate of high-cost deep geothermal wells, and the gas-fired boiler is usually used to take on peak load in the low-temperature geothermal central heating systems. In comparision to the gas-fired boiler, the gas-fired water/lithium bromide absorption heat pump has higher thermodynamic performance in the low-temperature sustainable central heating systems[20,21]. Thus, the gas-fired water/lithium bromide absorption heat pump would be a better choice to take on peak load in the low temperature geothermal central heating systems. However, for the deep hydrothermal type geothermal fields situated far away from center of heat load, the infrastructure of gas transmission and distribution is generally weak[22]. Constructing infrastructure of natural gas transportation network would bring greater initial investment capital, which results in higher non-energy cost. To improve economic benefit, constructing a new relay energy station based on natural gas would be a better choice nearby urban area. As for the conventional central heating systems, the relay energy station is used for pressure isolation and heat exchange between high-pressure network and low-pressure network, and the water-to-water heat exchanger is a current choice[23]. With regard to new relay energy station with the gas-fired water/lithium bromide absorption heat pump, system reconfiguration needs to be further studied.

The above problems considered, a new multi-energy source coupling a low temperature sustainable central heating system with a multifunctional relay energy station is put forward, and analyzed from the aspects of thermodynamic performance and economic benefit.

## 2. System descriotion

Sketch of the new low temperature sustainable central heating system is illustrated in **Figure 1**.

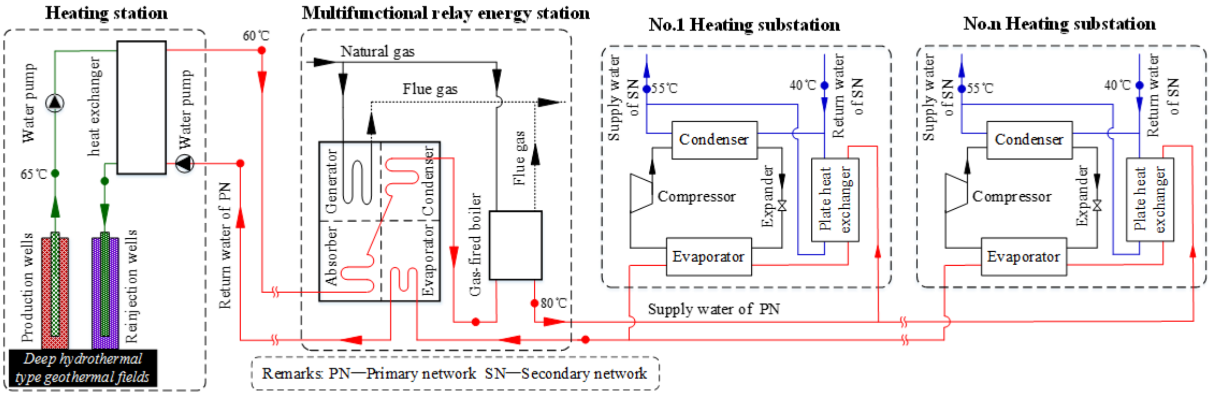


**Figure 1.** Sketch of the new low temperature sustainable central heating system.

## 2.1. Running principle of the heating station

The heating station mainly comprises production wells, reinjection wells, a heat exchanger, and two circulating water pumps.

In the heating station, geothermal water from the production wells comes into the heat exchanger, where it is used to heat return water of the primary network, and then it returns to the reinjection wells. At the same time, geothermal water is cooled by the return water of the primary network in the heat exchanger. Reinjection temperature of geothermal water mainly depends on return temperature of the primary network from the multifunctional relay energy station. In general, the low temperature return water of the primary network contributes to reducing temperature of injected geothermal water and utilizing low temperature geothermal energy efficiently.

## 2.2. Running principle of the multifunctional relay energy station

The multifunctional relay energy station is located nearby urban areas, and it is mainly made up of a gasfired water/lithium bromide single-effect absorption heat pump, and a gas-fired boiler.

In the multifunctional relay energy station, firstly, low temperature circulating water in the primary network from the heating substation comes into the evaporator of the gas-fired water/lithium bromide single-effect absorption heat pump, where it is further cooled by low-pressure refrigerant. Scondly, the heated circulating water in the primary network from the heating stations flows into the gas-fired water/lithium bromide single-effect absorption heat pump and the gas-fired boiler, where it is further heated.

It should be emphasized that, the gas-fired water/lithium bromide single-effect absorption heat pump plays two roles in the multifunctional relay energy station. One role is used to rise supply temperature of the primary network for covering the demand of peak load. Moreover, rising supply temperature of the primary network contributes to improving performance of the compression heat pumps in the heating substations. The other role is used to further lower return temperature of the primary network, which contributes to lowering reinjection temperature of geothermal water. Obviously, the roles played by the gas-fired water/lithium bromide single-effect absorption heat pump are more than that played by the gas-fired boiler in the multifunctional relay energy station.

## 2.3. Running principle of the heating substation

In the heating substation, a compression heat pump is coupled with a plate heat exchanger for lowering return temperature of the primary network. Circulating water in the secondary network is firstly split into two parts, and then two parts come into the plate heat exchanger and condenser of the compression heat pump respectively, where they are heated. Finally, the heated two parts converge, and serve as supply water of the secondary network. At the same time, the supply water of the primary network flows into the plate heat exchanger and evaporator of the compression heat pump in turn, and it is cooled step by step. In this way, the return temperature of the primary network is reduced step by step for big temperature difference between supply water and return water.

### 2.4. Characteristics of the new low temperature sustainable central heating system

For the new low temperature sustainable central heating system, location of the new multifunctional relay energy station is shown in **Figure 2**. It not only can be used to take on peak load, but can be also used to further lower temperature of return water for big temperature difference between supply water and return return of the primary network.

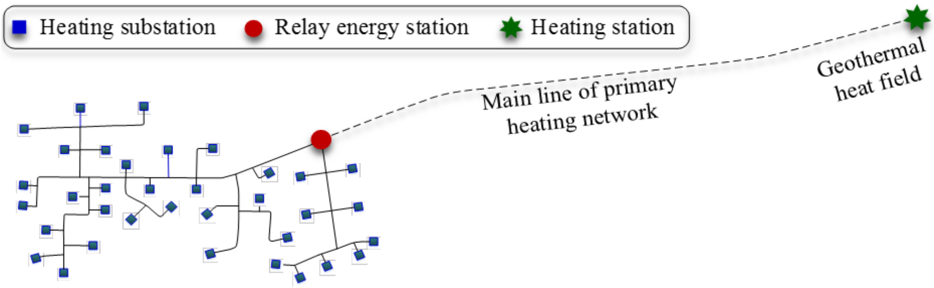


**Figure 2.** Topological graph of the primary network in the new low temperature sustainable central heating system.

The new low temperature sustainable central heating system is characterized by low design return temperature of the primary network, big temperature different between supply water and return water of the primary network, and multi-energy sources coupled operation.

## 3. Model construction

### 3.1. Model construction

(1) Current heat exchanger

Mathematic model of the current heat exchanger[24] is referred, and energy conservation equation of the current heat exchanger in the heating station is expressed as follows:

$$Q_{whe,hs} = m_{gw}\left(h_{gw,in} - h_{gw,out}\right) \tag{1}$$

where,

$Q_{whe,hs}$ = Heat transfer rate of the current heat exchanger in the heating station,

$m_{gw}$ = Mass flow rate of geothermal water,

$h_{gw,in}/h_{gw,out}$ = Specific enthalpy of geothermal water at the inlet/outlet.

As for the current plate heat exchanger in the heating substation, energy conservation equation is given as follows:

$$Q_{whe,hsb} = m_{1w}\left(h_{w1,in} - h_{w1,out}\right) \tag{2}$$

where,

$Q_{whe,hsb}$ = Heat transfer rate of the plate heat exchanger in the heating substation,

$m_{w1}$ = Mass flow rate of circulating water in the primary network,

$h_{w1,in}/h_{w1,out}$ = Specific enthalpy of circulating water at the inlet/outlet.

(2) Gas-fired water/lithium bromide single-effect absorption heat pump

Mathematic models of the gas-fired water/lithium bromide single-effect absorption heat pump[25,26] are considered, and its energy conservation equations can be written as follows:

$$Q_{ahp,gen} = \eta_{ahp} \times B_{ahp} \times h_{lcv,ng} \tag{3}$$

$$Q_{ahp,gen} + Q_{ahp,eva} = Q_{ahp,abs} + Q_{ahp,con} \tag{4}$$

$$COP_{ahp} = \left(Q_{ahp,abs} + Q_{ahp,con}\right)/Q_{ahp,gen} \tag{5}$$

where,

$Q_{ahp,gen}/Q_{ahp,eva}/Q_{ahp,abs}/Q_{ahp,con}$ = Generator capacity/evaporator capacity/absorber capacity/condenser capacity of the single-effect absorption heat pump,

$B_{ahp}$ = Consumtpion rate of natural gas,

$\eta_{w1}$ = Efficiency of calorific value for natural gas combustion,

$h_{lcv,ng}$ = Low calorific value of natural gas,

*COP* = Coefficient of performance of the single-effect absorption heat pump for heating.

(3) Gas-fired boiler

Mathematic model of the gas-fired boiler[26] is considered, and its energy conservation equations are expressed as follows:

$$Q_{ngb} = B \times h_{icv,ng} \times \eta_{ngb} \tag{6}$$

$$\eta_{ngb} = 0.0015Q_{ngb} + 0.8814 \tag{7}$$

$$Q_{ngb} = m_{w1}\left(h_{w1,ngb,out} - h_{w1,ahp,con,out}\right) \tag{8}$$

where,

$Q_{ngb}$ = Heating capacity of natural gas fired boiler,

$h_{w1,ngb,out}$ = Specific enthalpy of circulating water for the primary network at the outlet of natural gas fired boiler,

$h_{w1,ngb,out}$ = Specific enthalpy of circulating water for the primary network at the outlet of condenser in the absorption heat pump.

(4) Compression heat pump

Mathematic model of the compression heat pump[27–29] is referred. For one in the heating substation, energy conservation equations are given as follows:

$$N_{chp,com} = m_{r,chp}\left(h_{r,com,out} - h_{r,com,in}\right)/\eta_{com} \tag{9}$$

$$Q_{chp,con} = Q_{chp,eva} + N_{chp,com} \tag{10}$$

$$COP_{chp} = Q_{chp,con}/N_{chp,com} \tag{11}$$

where,

$N_{chp,com}$ = Power of compressor in compression heat pump,

$m_{r,chp}$ = Mass flow rate of refrigerant in compression heat pump,

$h_{r,com,in}/h_{r,com,out}$ = Specific enthalpy of refrigerant at the inlet/outlet of compressor,

$\eta_{1w}$ = Efficiency of compressor,

$Q_{chp,con}/Q_{chp,eva}$ = Condenser capacity/evaporator capacity of compression heat pump.

(5) Water pump

Power of water pump is determined as follows:

$$N_{wp} = \frac{m_{cw} \times \Delta P}{\rho_{cw} \times \eta_{wp}} \tag{12}$$

where,

$N_{wp}$ = Power of circulating water pump,

$m_{cw}$ = Mass flow rate of circulating water pump,

$\triangle P$ = pressure drop,

$\rho_{cw}$ = density of circulating water,

$\eta_{wp}$ = Efficiency of circulating water pump.

(6) Central heating system

During a whole heating period, heat output, geothermal energy input, power consumption, and consumption of natural gas are compulated as follows:

$$Qh_{ch} = \int_{t_0=t_1}^{t_0=t_2} m_{w2}\left[h_{w2,sup}(t_0) - h_{w2,ret}(t_0)\right]d\tau(t_0) \tag{13}$$

$$Qh_{gw} = \int_{t_0=t_1}^{t_0=t_2} m_{gw}(t_0)\left[h_{gw,in}(t_0) - h_{gw,out}(t_0)\right]d\tau(t_0) \tag{14}$$

$$EC_{ch} = \int_{t_0=t_1}^{t_0=t_2} \left[N_{gw,wp}(t_0) + N_{1w,wp}(t_0) + N_{2w,wp}(t_0) + N_{chp,com}(t_0)\right]d\tau(t_0) \tag{15}$$

$$NGC_{ch} = \int_{t_0=t_1}^{t_0=t_2} \left[B_{ahp}(t_0) + B_{ngb}(t_0)\right]d\tau(t_0) \tag{16}$$

where,

$Qh_{ch}$ = Output heat of central heating system during a whole heating period,

$m_{w2}$ = Mass flow rate of circulating water in the secondary network,

$h_{w2,sup}/h_{w2,ret}$ = Specific enthalpy of supply water / return water of the secondary network,

$\tau(t_0)$ = Time of duration for specific outdoor air temperature,

$t_0$ = Outdoor air temperature,

$Qh_{gw}$ = Output of gepthermal energy during a whole heating period,

$EC_{ch}$ = Electricity consumption of central heating system during a whole heating period,

$NGC_{ch}$ = Natural gas consumption of central heating system during a whole heating period.

## 3.2. Evaluation indicators

With regard to the new low temperature sustainable central heating system, system performance would vary with the rising of outdoor air temperature. Therefore, system performance of the new low temperature sustainable central heating system must be evaluated from the perspective of a whole heating period[30], and annual energy efficiency of fossil fuel (AEEFF) and annual product exergy efficiency (APEE) are put forward. AEEFF is defined as the ratio of heat output to consumption of natural gas during a whole heating period, and it is compulated as follows:

$$AEEFF = \frac{Qh_{ch}}{BC_{ch} + \gamma \times EC_{ch}} \tag{17}$$

where,

$Qh_{dh}$ = Output heat of central heating system during a whole heating period.

$\gamma$ = average conversion rate of natural gas to electricity, and it is about 39.3% according to statistical data of the existing gas-fired power plants[10,31]. Exergy is defined as the maximum amount of work for a stream of energy flow, and it can be taken as a measure of energy quality. APEE is defined to be the ratio of product exergy output of the secondary network to the sum of exergy inputs of geothermal water, power and chemical exergy of natural gas during a heating period, and its compulation formula is given as follows:

$$PEE = \frac{\int m_{w2}\left[e_{w2,out}(t_0) - e_{w2,in}(t_0)\right]d\tau(t_0)}{\int m_{gw}\left[e_{gw,in}(t_0) - e_{gw,out}(t_0)\right]d\tau(t_0) + \int\left[B(t_0) \times e_{ch} - m_{fg}(t_0) \times e_{fg}\right]d\tau(t_0) + EC_{dh}} \quad (18)$$

where,

$e_{w2,out}$/$e_{w2,in}$ = Specific exergy of circulating water in the secondary network at the inlet/outlet,

$e_{gw,out}$/$e_{gw,in}$ = Specific exergy of geothermal water at the inlet/outlet,

$e_{ch}$ = Chemical exergy of natural gas,

$e_{fg}$ = Specific exergy of flue gas.

# 4. Analysis of Case

The case is located in Northern China, and its heat load and running period are 200 MW and 123 days. Depths of geothermal wells are about 3000 meters, and outlet temperature of geothermal water is 65 ℃.

## 4.1. Main information

For the new low temperature sustainable central heating system, some information is given as follows:

1) Heat loss of the central heating system is compulated by 5.0% of heat load[32].
2) For compression heat pump with R134a in heating substation, compressor's efficiency is 81%[33].
3) Calcuation of specific exergy is referred to −9.0 ℃ and 101,325 Pa.
4) Prices of power, natural gas and heating are 0.7995 ¥/kWh, 2.36 ¥/Nm$^3$ and 30 ¥/m$^2$.
5) low-calorific value of natural gas is 34.59 MJ/Nm$^3$.
6) Pressure loss per kilometer is 66,000 Pa for the primary network.
7) Annual interest rate adopts 4.8%.
8) For hydrothermal type geothermal resource, tax adopts 1 ¥/m$^3$[34].
9) To improve performance of compression heat pump, operation modes of both the primary network and the secondary network adopt constant mass flow rate[17].

In general, low return temperature of the primary network contributes to utilizing low-temperature hydrothermal type geothermal energy efficiently, but it would result in more electricity consumption of the compression heat pumps in the heating substations. Thus, there is an optimal design return temperature of the primary network. To analyze impacts of the design return temperature of the primary network on performance of the new low temperature sustainable central heating system, four schemes with different design return temperature of the primary network are presented according to both design guidance principles of central heating and operational characteristics of compression heat pump, and their main thermal parameters are given in **Table 1**.

As is shown in **Table 1**, design return temperature of the primary network can approach 13 ℃ by using compression heat pumps integrated with plate heat exchangers in the heating substation and the gas-fired water/lithium bromide single-effect absorption heat pump in the multifunction relay energy station. With design return temperature of the primary network decreasing, heating capacity of the deep hydrothermal type geothermal wells becomes large.

As outdoor air temperature rises, difference between outdoor air temperature and indoor air temperature will becomes small, and thus heat loss of the buildings is reduced accordingly. Thus, the demand of heat load becomes large, and both the gas-fired water/lithium bromide single-effect absorption heat pump and the gas-fired boiler will be put into operation in turn. Variation curve of heat load for the case is shown in **Figure 3**.

**Table 1.** Main thermal parameters of four schemes for the new low temperature sustainable central heating system.

| Subsystem | Equipment | Item | Scheme A | Scheme B | Scheme C | Scheme D |
|---|---|---|---|---|---|---|
| Heating station | Heat exchanger | Design temperature of return water of PN (°C) | 13.0 | 18.0 | 23.0 | 28.0 |
| | | Outlet temperature of circulating water in PN (°C) | 60.0 | 60.0 | 60.0 | 60.0 |
| | | Capacity of heat transfer (kW) | 1,478,489 | 1,469,519 | 144,089 | 140,305 |
| | | Outlet temperature of geothermal wate r (°C) | 65.0 | 65.0 | 65.0 | 65.0 |
| | | Reinjection temperature of geothermal water (°C) | 35.4 | 35.5 | 36.1 | 38.0 |
| | | Mass flow rate of geothermal water (kg/s) | 1191.75 | 1191.75 | 1191.75 | 1191.75 |
| Primary network (PN) | - | Mass flow rate of circulating water (kg/s) | 751.81 | 836.23 | 946.73 | 1061.99 |
| Multifunction relay energy station | Gas-fired water/lithium bromide absorption heat pump | Outlet temperature of circulating water from condenser (°C) | 76.6 | 78.8 | 78.6 | 78.4 |
| | | Outlet temperature of circulating water from evaporator (°C) | 13.0 | 18.0 | 23.0 | 28.0 |
| | | COP (kW/kW) | 1.731 | 1.593 | 1.602 | 1.615 |
| | | Heating capacity (kW) | 285,049 | 387,279 | 43,202 | 47,486 |
| | Gas-fired boiler | Design temperature of supply water in PN (°C) | 80.0 | 80.0 | 80.0 | 80.0 |
| | | Heating capacity (kW) | 12,426 | 6928 | 8239 | 10,313 |
| Heating substation | Compression heat pump | Outlet temperature of circulating water in PN (°C) | 20.0 | 25.0 | 30.0 | 35.0 |
| | | Outlet temperature of circulating water in SN (°C) | 48.2 | 47.2 | 46.0 | 44.2 |
| | | Discharge pressure of compressor (Pa) | 1,360,000 | 1,325,000 | 1,282,000 | 1,228,000 |
| | | Suction pressure of compressor (Pa) | 520,900 | 608,300 | 706,300 | 815,900 |
| | | Power (kW) | 11,222 | 7522 | 4370 | 1897 |
| | | Heating capacity (kW) | 83,590 | 70,509 | 55,546 | 37,116 |
| | Plate heat exchanger | Outlet temperature circulating water in PN (°C) | 43.0 | 43.0 | 43.0 | 43.0 |
| | | Inlet temperature of circulating water in SN (°C) | 77.0 | 77.0 | 77.0 | 77.0 |
| | | Heating capacity (kW) | 116,410 | 129,491 | 144,454 | 162,884 |
| Secondary network (SN) | - | Design temperature of supply water (°C) | 55.0 | 55.0 | 55.0 | 55.0 |
| | | Design temperature of return water (°C) | 40.0 | 40.0 | 40.0 | 40.0 |
| | | Mass flow rate of circulating water (kg/s) | 3185.98 | 3185.98 | 3185.98 | 3185.98 |

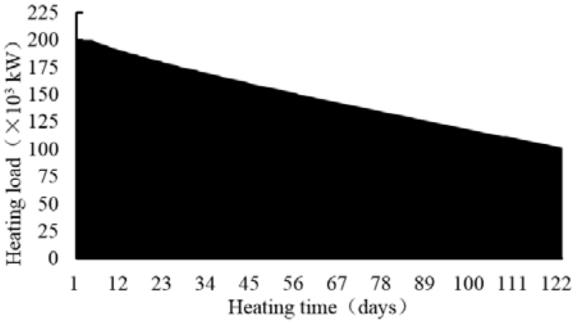


**Figure 3.** Variation curve of heating load for the case.

## 4.2. Thermodynamic performance

For the new low temperature sustainable central heating system, long main line of the primary network generally results in more power consumption of circulating water pumps, and thus it would have an impact on both annual energy efficiency of fossil fuel and annual product exergy efficiency.

For the four schemes, relationships between main line length of the primary network and annual energy efficiency of fossil fuel are illustrated in **Figure 4**.

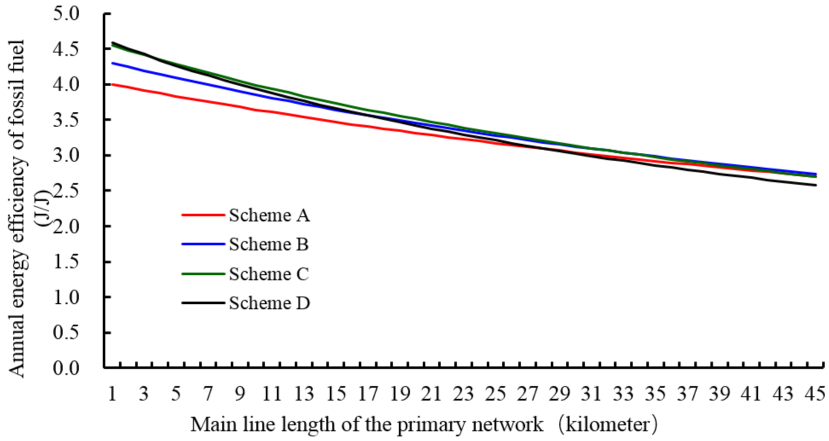


**Figure 4.** Relationships between AEEFF and main line length of the primary network.

It can be seen from **Figure 4** that, AEEFF of the four schemes decrease with the increase of main line length of the primary network, and the impact of main line length of the primary network on AEEFF for the scheme A is the smallest among that of the four schemes. This is caused by the fact that, as design return temperature of the primary network becomes low, the increase value of power consumption of compression heat pumps in the heating substations is bigger than the decrease value of power consumption of circulating water pumps in the primary network, especially for small main line length of the primary network. When main line length of the primary network is smaller than 2.9 km, the ranking of the four schemes by AEEFF is scheme D > scheme C > scheme B > scheme A. When main line length of the primary network is bigger than 2.9 km and smaller than 34.0 km, annual energy efficiency of fossil fuel for the scheme C is the biggest among that of the four schemes. When main line length of the primary network is bigger than 34.0 km and smaller than 45.0 km, AEEFF for the scheme B is the biggest among that of the four schemes.

From the perspective of AEEFF, there in an optimal matching relationship between design return temperature and main line length of the primary network in the new low temperature sustainable central heating system. As for the primary network, optimal design temperature of return water becomes low with the increase of main line length.

For the four schemes, relationships between main line length of the primary network and annual product exergy efficiency are exhibited in **Figure 5**.

**Figure 5** indicates that, as for the four schemes, APEE becomes smaller with main line of the primary network becoming longer, and lowering design return temperature of the primary network contributes to improving APEE for the new low temperature sustainable central heating system. The reason is that low design return temperature of the primary network helps to utilize low temperature geothermal energy efficiently, and it would results in reduction of natural gas consumption. Moreover, comparing with natural gas, low temperature geothermal water is suitable for space heating from the aspect of energy grade matching. For the new low temperature sustainable central heating system, the ranking of the four schemes by APEE is scheme A > scheme B > scheme C > scheme D.

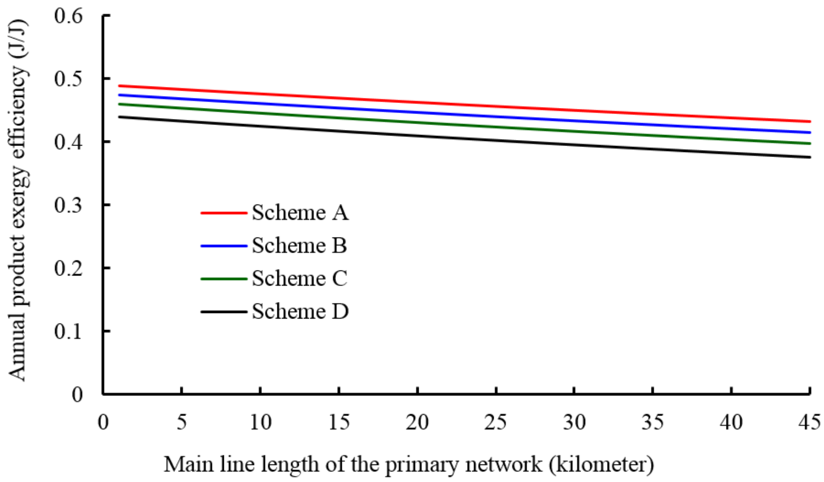


**Figure 5.** Relationships between APEE and main line length of primary network.

### 4.3. Economic benefit

Initial investment capital is usually splited into equipment cost, construction cost, installment cost and other cost. The equipment cost is compulated by current price in market for specific equipment in China, and other cost is compulated according to requirements of China's current investment estimation standard for public works[35]. For the clean energy central heating systems, government's subsidy would be provided according to 50% of initial investment capital[36]. When main line length of the primary network is 20 km, the initial investment capitals of the four schemes are illustrated in **Table 2**.

**Table 2.** Initial investment capitals of four schemes.

| Subsystem | Item | Scheme A | Scheme B | Scheme C | Scheme D |
|---|---|---|---|---|---|
| Heating station | Wells drilling cost (¥) | 271,422,700 | 271,422,700 | 271,422,700 | 271,422,700 |
| | Equipment cost (¥) | 45,413,100 | 45,144,200 | 43,226,600 | 42,091,400 |
| | Construction cost (¥) | 6,812,000 | 6,771,600 | 6,484,000 | 6,313,700 |
| | Installation cost (¥) | 9,082,600 | 9,028,800 | 8,645,300 | 8,418,300 |
| | Other cost (¥) | 6,812,000 | 6,771,600 | 6,484,000 | 6,313,700 |
| Multifunction relay energy station | Equipment cost (¥) | 30,205,200 | 30,856,300 | 35,182,300 | 39,861,000 |
| | Construction cost (¥) | 4,530,800 | 4,628,500 | 5,277,300 | 5,979,200 |
| | Installation cost (¥) | 6,041,100 | 6,171,300 | 7,036,500 | 7,972,200 |
| | Other cost (¥) | 4,530,800 | 4,628,500 | 5,277,300 | 5,979,200 |
| Primary network (Main line length of 20 km) | Pipelines cost (¥) | 56,814,900 | 59,305,300 | 62,371,500 | 65,375,600 |
| | Construction cost (¥) | 55,546,600 | 57,334,700 | 59,550,400 | 61,735,400 |
| | Installation cost (¥) | 52,000,000 | 52,000,000 | 52,000,000 | 52,000,000 |
| | Other cost (¥) | 25,511,600 | 26,133,700 | 26,897,700 | 27,643,800 |
| Heating substation | Equipment cost (¥) | 47,801,800 | 44,426,100 | 39,893,400 | 33,886,900 |
| | Construction cost (¥) | 7,170,300 | 6,663,900 | 5,984,000 | 5,083,000 |
| | Installation cost (¥) | 9,560,400 | 8,885,200 | 7,978,700 | 6,777,400 |
| | Other cost (¥) | 7,170,300 | 6,663,900 | 5,984,000 | 5,083,000 |
| Heating system | Total first cost (¥) | 646,426,200 | 646,836,300 | 649,695,700 | 651,936,500 |
| | Government subsidy (¥) | 279,770,600 | 266,945,000 | 286,130,000 | 270,657,300 |

Remarks: 1 € = 6.9544 ¥ and 1 $ = 6.9266 ¥.

**Table 2** shows that first cost of drilling geothermal well is a main component of total initial investment capitial for the four schemes. Besides, construction cost increases with the design return temperature of the primary network rising for the new low temperature sustainable central heating system.

Investment recovery period is usually used to assess economic benefit of the central heating systems. For the new low temperature sustainable central heating system, heating cost can be divided into energy cost and non-energy cost. The energy cost comprises electricity cost, natural gas cost, and tax fee of geothermal resource. The non-energy cost consists of maintenance cost, amortization cost of fixed equipment, and labor fee. For a fixed equipment, amortization cost (*AC*) is compulated over its life cycle as follows:

$$AC = FAC \times \frac{i \times (1+i)^n}{(1+i)^n - 1} \tag{19}$$

where, *n* is taken as 40 for the primary and secondary networks, 30 for the geothermal wells, and 15 for other equipment. The life cycles of heating network, geothermal well and equipment are referred to safety management regulation of central heating system and product manuals of current thermal equipment in China.

For the primary network, main line length generally affects both initial investment capital and power consumption of circulating water pump, and thus it would have an impact on investment recovery period of the four schemes. For the four schemes, variation curves of investment recovery period are indicated in **Figure 6**.

It can be found from **Figure 6** that, as main line length of the primary network is within the range from 1.0 km to 35.2 km, investment recovery period of the scheme C is the shortest among that of the four schemes. As main line length of the primary network is bigger than 35.2 km and smaller than 45.0 km, investment recovery period of the scheme A is the shortest among that of the four schemes. According to benchmark of investment recovery period at 10 years, the cost-effective main line length of the primary network is about 33.6 km for the scheme A, about 32.5 km for the scheme B, about 33.8 km for the scheme C, and about 28.7 km for the scheme D. Among the four schemes, the scheme C has the longest cost-effective main line of the primary network. Therefore, from the aspect of investment recovery period, the ranking of the four schemes is scheme C > scheme A > scheme B > scheme D for the new low temperature sustainable central heating system with long main line of the primary network.

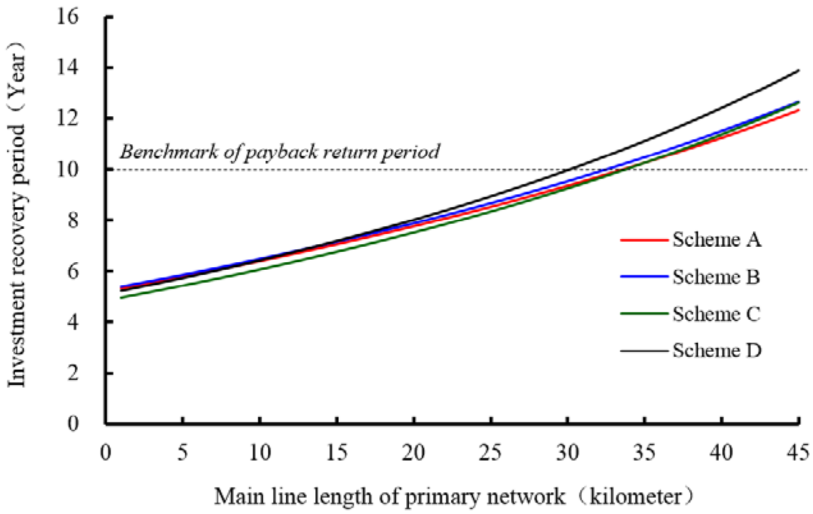


**Figure 6.** Variation curves of investment recovery period for the four schemes.

When main line length of the primary network is 33.8 km, structures of heating cost for the four schemes are illustrated in **Figure 7**.

**Figure 7** depicts that energy cost is about 50% of heating cost, and heating cost of the scheme B is the smallest among that of the four schemes. Heating cost of the scheme B is smaller about 4.60 ¥/GJ than that of the scheme A, about 0.35 ¥/GJ than that of the scheme C, and 1.33 ¥/GJ than that of the scheme D.

From the aspect of economic benefit, the scheme B would be a better choice for the new low temperature sustainable central heating system when main line length of the primary network is bigger than 33.8 km.

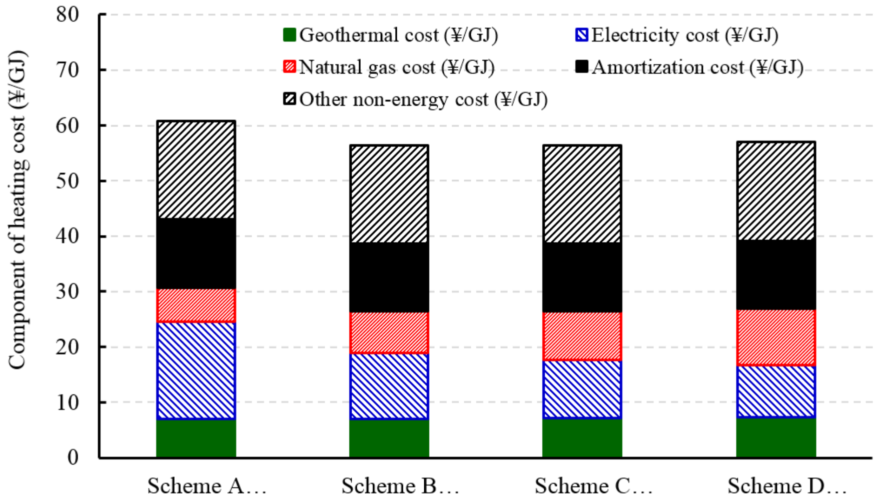


**Figure 7.** Structures of heating cost for the four schemes.

## 4.4. Potential of emission-reduction

When main line length of the primary network is 33.8 km, structures of energy consumption for the four schemes are shown in **Figure 8**.

**Figure 8** illustrates that, with the rising of design return temperature of the primary network, the amounts of both geothermal energy utilization and electricity consumption become small, but the amount of natural gas consumption becomes larger. Thus, lowering design return temperature of the primary network helps to reduce natural gas consumption through utilizing more geothermal energy. In comparison to the current gas-fired central heating system[16], the new low temperature sustainable central heating system can decrease natural gas consumption by about 9.0 $Nm^3$ for unit floor area during a whole heating period.

When main line length of the primary network is 33.8 km, structures of power consumption for the four schemes are illustrated in **Figure 9**.

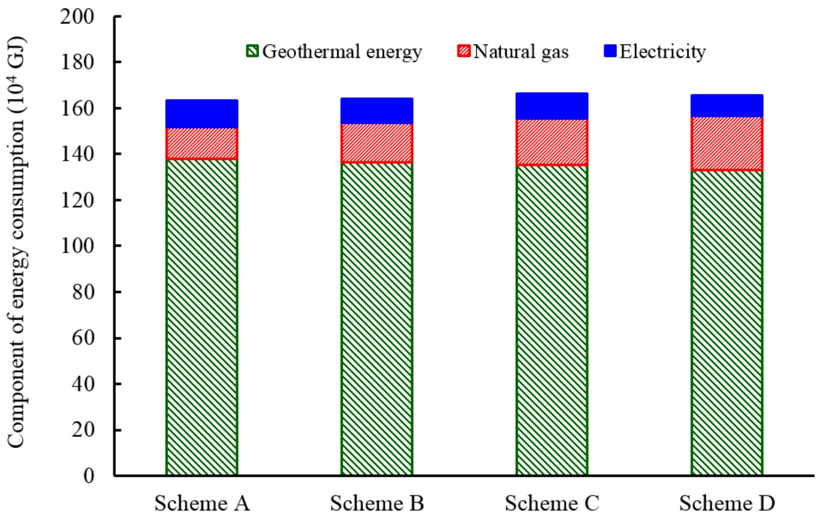


**Figure 8.** Structures of energy consumption for the four schemes.

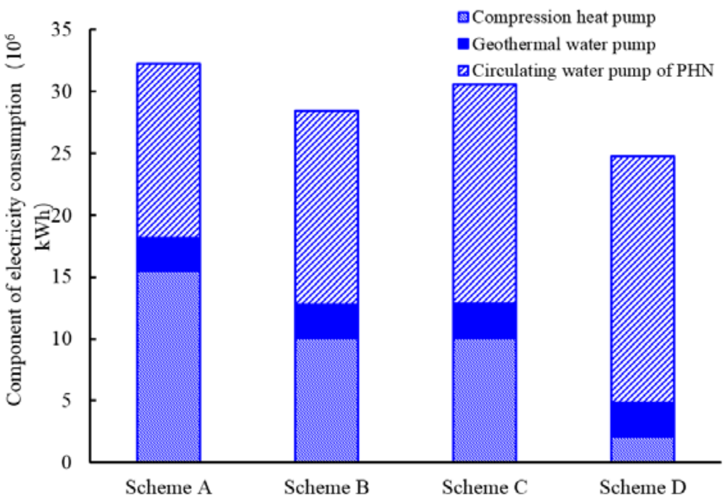


**Figure 9.** Structures of power consumption for the four schemes.

**Figure 9** shows that for the four schemes, electricity consumption of circulating water pump in the primary network is a major component of total electricity consumption. Amount of total electricity consumption of the scheme B is smaller than that of the scheme C and A, but it is larger than that of the scheme D. For the scheme B, the electricity consumption amount of compression heat pumps in the heating substations is about 55.1% of total electricity consumption amount. For the scheme D, electricity consumption amount of circulating water pump in the primary network is about 80.3% of total electricity consumption amount. It is caused by the fact that small temperature difference between supply water and return water of the primary network results in large mass flow rate of circulating water, and electricity consumption amount of water pump increases sharply for the new low temperature sustainable central heating system with long distance for transporting geothermal energy. Besides, low design return temperature of the primary network contributes to utilizing geothermal energy efficiently. Thus, lowering design return temperature of the primary network is a key measure to reduce consumption of electricity and natural gas for the new low temperature sustainable central heating system with long main line of the primary network.

Due to great saving potential of natural gas and electricity, the four schemes have geat potential of emission reduction of atmospheric pollutants correspondingly. Compared with the current natural gas-fired central heating systems, the four schemes can save a great deal of natural gas, and potentials of emission reductions of main atmospheric pollutants are given in **Table 3**.

**Table 3.** Emission reductions of main atmospheric pollutants for the four schemes.

| Scheme | Scheme A | Scheme B | Scheme C | Scheme D |
|---|---|---|---|---|
| Soot (ton) | 9.585 | 9.560 | 9.503 | 9.361 |
| $SO_x$ (ton) | 3.994 | 3.984 | 3.960 | 3.900 |
| $NO_x$ (ton) | 25.159 | 25.096 | 24.946 | 24.571 |
| $CO_x$ (ton) | 85,685.314 | 85,470.519 | 84,959.607 | 83,683.027 |

**Table 3** indicates that, when main line length of the primary network is 33.8 km, the ranking of the four schemes by potential of emission reductions of main atmospheric pollutants is scheme A > scheme B > scheme C > scheme D. The reason is that low design return temperature of the primary network helps to reduce consumption of natural gas.

## 5. Conclusion

The new low temperature sustainable central heating system is studied from the perspectives of thermodynamics and economics, and matching relationships between design return temperature and cost-effective main line length of the primary network are discussed. Following important conclusions are summarized.

1) The new low temperature sustainable central heating system can achieve design return temperature of the primary network at 13 °C by using compression heat pumps in the heating substations and the gas-fired water/lithium bromide single-effect absorption heat pump in the new multifunctional relay energy station.

2) In the new multifunctional relay energy station located nearby urban area, the gas-fired water/lithium bromide single-effect absorption heat pump not only can take on peak load by about 14%, but can also lower return temperature of the primary network by about 7 °C. Comparing with the gas-fired boiler, the gas-fired water/lithium bromide single-effect absorption heat pump can play more roles in the new low temperature sustainable central heating system.

3) For the new low temperature sustainable central heating system with geothermal water temperature at 65 °C, there is an optimal matching relationship between cost-effective main line length of the primary network and design return temperature of the primary network. Concerning design return temperature of the primary network, 28 °C is suitable for main line length of the primary network within the range from 1.0 km to 2.9 km, and 23 °C is suitable for main line ength of the primary network within the range from 2.9 km to 33.8 km.

4) For the new low temperature sustainable central heating system, the cost-effective main line length of the primary network is about 33.8 km, and its annual energy efficiency of fossil fuel and annual product exergy efficiency are about 3.01 and 42.7%, respectively. Thus, the new low temperature sustainable central heating system has an advanced energy conversion and transfer process.

5) The new low temperature sustainable central heating system is characterized by high thermodynamic performance, good economic benefit, and long cost-effective distance for transmitting geothermal energy, and thus its application is promising in Northern China.

## Author contributions

Conceptualization, FS; methodology, FS; validation, YX; formal analysis, XZ; modification, XZ; simulation and data process, WX; writing—review and editing, ZW; model construction, YX; supervision, FS; project administration, Beijing University of Civil Engineering and Architecture; funding acquisition, Beijing Natural Science Foundation (3222027). All authors have read and agreed to the published version of the manuscript.


## Funding

This research was funded by Beijing Natural Science Foundation, grant number 3222027.


## Conflict of interest

The authors declare no conflict of interest.

## Abbreviations

| | | | |
|---|---|---|---|
| *COP* | coefficient of performance, W/W | gw | geothermal water |
| *Q* | heating capacity, W | in | inlet |
| *m* | mass flow rate, kg/s | out | outlet |
| *h* | specific enthalpy, J/kg | w1 | water in the primary heating network |

| | | | |
|---|---|---|---|
| $\eta$ | efficiency | ahp | absorption heat pump |
| $B$ | natural gas consumption rate, kg/s | lcv | low calorific value |
| $N$ | power, W | ng | natural gas |
| $\rho$ | density, kg/m$^3$ | gen | generator |
| $\Delta P$ | pressure drop, Pa | eva | evaporator |
| $Qh$ | thermal energy, J | abs | absorber |
| $T/t$ | temperature, K/°C | con | condenser |
| $\tau$ | time, second | ngb | natural gas boiler |
| EC | electricity consumption, J | chp | electric compression heat pump |
| NGC | natural gas consumption, m$^3$ | r | refrigerant |
| $e$ | specific exergy, J/kg | com | compressor |
| AEEFF | annual energy efficiency of fossil fuel | wp | water pump |
| $\gamma$ | conversion rate of gas to electricity | cw | circulating water |
| APEE | annual product exergy efficiency | ch | district heating |
| AC | amortization cost | sup | supply |
| FAC | fixed asset cost | ret | return |
| $i$ | annual interest rate | o | outdoor air temperature |
| $n$ | number | w2 | water in the secondary heating network |
| Sub | super-scripts | PN | primary network |
| hs | heating station | SN | secondary network |
| whe | water-to-water heat exchanger | | |

## References


1. Gjoka K, Rismanchi B, Crawford RH. Fifth-generation district heating and cooling systems: A review of recent advancements and implementation barriers. *Renewable and Sustainable Energy Reviews* 2023; 171: 112997. doi: 10.1016/j.rser.2022.112997
2. Sorknæs P, Nielsen S, Lund H, et al. The benefits of 4th generation district heating and energy efficient datacenters. *Energy* 2022; 260: 125215. doi: 10.1016/j.energy.2022.125215
3. Wang G, Liu Y, Zhu X, Zhang W. The status and development trend of geothermal resources in China. *Earth Science Frontiers* 2020; 27(1): 1–9. doi: 10.13745/j.esf.2020.1.1
4. Molar-Cruz A, Keim MF, Schifflechner C, et al. Techno-economic optimization of large-scale deep geothermal district heating systems with long-distance heat transport. *Energy Conversion and Management* 2022; 267: 115906. doi: 10.1016/j.enconman.2022.115906
5. Limberger J, Boxem T, Pluymaekers M, et al. Geothermal energy in deep aquifers: A global assessment of the resource base for direct heat utilization. *Renewable and Sustainable Energy Reviews* 2018; 82(Part 1): 961–975. doi: 10.1016/j.rser.2017.09.084
6. Bai J, Jia W, Liu L. Research on the application and development potential of middle and deep geothermal heating technology in Beijing heating market. *Heating Ventilating & Air conditioning* 2017; 47: 43–47.
7. Building Energy Research Center of Tsinghua University. In: *Annual Report of China Building Energy Conservation 2023* (Chinese). Architecture and Building Press; 2023. pp.267–278.
8. Sun F, Hao B, Fu L, et al. New medium-low temperature hydrothermal geothermal district heating system based on distributed electric compression heat pumps and a centralized absorption heat transformer. *Energy* 2021; 232: 120974. doi: 10.1016/j.energy.2021.120974
9. Sun F, Zhao X, Chen X, et al. New configurations of district heating system based on natural gas and deep geothermal energy for higher energy efficiency in northern China. *Applied Thermal Engineering* 2019; 151: 439–450. doi: 10.1016/j.applthermaleng.2019.02.043
10. Li Y, Pan W, Xia J, Jiang Y. Combined heat and water system for long-distance heat transportation. *Energy* 2019; 172: 401–408. doi: 10.1016/j.energy.2019.01.139
11. Fu L, Li Y, Wu Y, et al. Low carbon district heating in China in 2025—A district heating mode with low grade waste heat as heat source. *Energy* 2021; 230: 120765. doi: 10.1016/j.energy.2021.120765

12. Li Y, Xia J, Su Y, Jiang Y. Systematic optimization for the utilization of low-temperature industrial excess heat for district heating. *Energy* 2018; 144: 984–991. doi: 10.1016/j.energy.2017.12.048
13. Xie X, Jiang Y. Absorption heat exchangers for long-distance heat transportation. *Energy* 2017; 141: 2242–2250. doi: 10.1016/j.energy.2017.11.145
14. Mirl N, Schmid F, Spindler K. Reduction of the return temperature in district heating systems with an ammonia-water absorption heat pump. *Case Studies in Thermal Engineering* 2018; 12: 817–822. doi: 10.1016/j.csite.2018.10.010
15. Sun f, Chen X, Fu L, Zhang S. Configuration optimization of an enhanced ejector heat exchanger based on an ejector refrigerator and a plate heat exchanger. *Energy* 2018; 164: 408–417. doi: 10.1016/j.energy.2018.08.194
16. Sun F, Hao B, Fu L, et al. New medium-low temperature hydrothermal geothermal district heating system based on distributed electric compression heat pumps and a centralized absorption heat transformer. *Energy* 2021; 232: 120974. doi: 10.1016/j.energy.2021.120974
17. Sommer T, Sotnikov A, Sulzer M, et al. Hydrothermal challenges in low-temperature networks with distributed heat pumps. *Energy* 2022; 257: 124527. doi: 10.1016/j.energy.2022.124527
18. Schlosser F, Jesper M, Vogelsang J, et al. Large-scale heat pumps: Applications, performance, economic feasibility and industrial integration. *Renewable and Sustainable Energy Reviews* 2020; 133: 110219. doi: 10.1016/j.rser.2020.110219
19. Osterman E, Stritih U. Review on compression heat pump systems with thermal energy storage for heating and cooling of buildings. *Journal of Energy Storage* 2021; 39: 102569. doi: 10.1016/j.est.2021.102569
20. Herold KE, Radermacher R, Klein SA. *Absorption Chillers and Heat Pumps*, 2nd ed. CRC press; 2016. pp. 173–177.
21. Lu D, Chen G, Gong M, et al. Thermodynamic and economic analysis of a gas-fired absorption heat pump for district heating with cascade recovery of flue gas waste heat. *Energy Conversion and Management* 2019; 185: 87–100. doi: 10.1016/j.enconman.2019.01.110
22. Dong J, Sha S, Li X, et al. Ownership unbundling of natural gas transmission networks in China. *Journal of Cleaner Production* 2018; 195: 145–153. doi: 10.1016/j.jclepro.2018.05.173
23. Chen P, Kedan Ji. Analysis on heat transfer performance of large-scale plate heat exchanger in Taigu relay energy station (Chinese). *District Heating* 2019; 77–81. doi: 10.16641/j.cnki.cn11-3241/tk.2019.01.012
24. Browne MW, Bansal PK. An elemental NTU-ε model for vapour-compression liquid chillers. *International Journal of Refrigeration* 2001; 24: 612–627. doi: 10.1016/S0140-7007(00)00091-8
25. Sun J, Fu L, Zhang S, Hou W. A mathematical model with experiments of single effect absorption heat pump using LiBr-$H_2O$. *Applied Thermal Engineering* 2010; 30(17–18): 2753–2762. doi: 10.1016/j.applthermaleng.2010.07.032
26. Wu Z, You S, Zhang H, et al. Performance analysis and optimization for a novel air-source gas-fired absorption heat pump. *Energy Conversion and Management* 2020; 223: 113423. doi: 10.1016/j.enconman.2020.113423
27. Ciampi G, Rosato A, Sibilio S. Thermo-economic sensitivity analysis by dynamic simulations of a small Italian solar district heating system with a seasonal borehole thermal energy storage. *Energy* 2018; 143: 757–771. doi: 10.1016/j.energy.2017.11.029
28. Liu J, Li Q, Wang F, Zhou L. A new model of screw compressor for refrigeration system simulation. *International Journal of Refrigeration* 2012; 35(4): 861–870. doi: 10.1016/j.ijrefrig.2012.01.016
29. Yu FW, Chan KT. Improved energy performance of air cooled centrifugal chillers with variable chilled water flow. *Energy Conversion and Management* 2008; 49(6): 1595–1611. doi: 10.1016/j.enconman.2007.12.009
30. Dorotic H, Puksec T, Duic N. Multi-objective optimization of district heating and cooling systems for a one-year time horizon. *Energy* 2019; 169: 319–328. doi: 10.1016/j.energy.2018.11.149
31. Gonzalez-Salazar MA, Kirsten T, Prchlik L. Review of the operational flexibility and emissions of gas- and coal-fired power plants in a future with growing renewables. *Renewable and Sustainable Energy Reviews* 2018; 82, Part 1: 1497–1513. doi: 10.1016/j.rser.2017.05.278
32. Ministry of Housing and Urban-Rural Development of the People’s Republic of China (MOHURD). *Industry Standard of The People’s Republic Of China: Design Code For City Heating Network (CJJ 34-2010)* (Chinese). China’s Architecture and Building Press; 2010.
33. Ahamed JU, Saidur R, Masjuki HH. A review on exergy analysis of vapor compression refrigeration system. *Renewable and Sustainable Energy Reviews* 2011; 15: 1593–1600. doi: 10.1016/j.rser.2010.11.039
34. Standing committee of the National People’s Congress. Resource Tax Law of the People’s Republic of China, 2022 (Chinese). Available online: http://jdjc.mof.gov.cn/fgzd/202201/t20220106_3781190.htm (accessed on 27 July 2023).
35. Standard fixed institute of Ministry of Housing and Urban-Rural Development of the People’s Republic of China. *Indicators of Investment in Public Works Estimates* (Chinese). China’s Planning Press; 2007.
36. People’s Government of Beijing Municipality. *Implementation Opinions on Further Accelerating the Application of Clean District Heating Integrated with Heat Pump* (Chinese). People’s Government of Beijing Municipality; 2019.